

A Correspondence between Phenomenological and $IBM - 1$ Models of Even Isotopes of Yb

Abdurahim Okhunov^{1,4}, Fadhil I. Sharrad², and Anwer A. Al-Sammarea^{3,5}

¹ Department of Science in Engineering, Faculty of Engineering
International Islamic University Malaysia
P.O. Box 10, 50728 Kuala Lumpur, Selangor, Malaysia
abdurahimokhun@iiu.edu.my

² Department of Physics, College of Science University of Kerbala, Karbala, Iraq

³ Department of Chemistry, College of Education, Faculty of Science
University of Samara, Selah, Iraq

⁴ Institute of Nuclear Physics, Academy of Science Republic of Uzbekistan
100214 Ulugbek, Tashkent, Uzbekistan

⁵ Quantum Science Centre, Department of Physics, Faculty of Science
University of Malaya, 50603 Kuala Lumpur, Malaysia

Abstract. This paper studies the nonterminal complexity of weakly conditional grammars, and it proves that every recursively enumerable language can be generated by a weak conditional grammar with no more than *seven* nonterminals. Moreover, it is shown that the number of nonterminals in weakly conditional grammars without erasing rules leads to an infinite hierarchy of families of languages generated by weakly conditional grammars.

Energy levels and the reduced probability of $E2^-$ transitions for Ytterbium isotopes with proton number $Z = 70$ and neutron numbers between 100 and 106 have been calculated through phenomenological (PhM) and interacting boson ($IBM - 1$) models. The predicted low-lying levels (energies, spins and parities) and the reduced probability for $E2^-$ transitions

results are reasonably consistent with the available experimental data. The predicted low-lying levels ($gr-$, β_1- and γ_1- band) by produced in the PhM are in good agreement with the experimental data comparison with those by $IBM - 1$ for all nuclei of interest. In addition, the phenomenological model was successful in predicted the β_2- , β_3- , β_4- , γ_2- and 1^+- band while it was a failure with $IBM - 1$. Also, the 3^+- band is predicted by the $IBM - 1$ model for ^{172}Yb and ^{174}Yb nuclei. All calculations are compared with the available experimental data.

Keywords : Ytterbium (Yb); Energy levels; model; even-even; isotopes; nuclei

PACS No. : 21.10.-k, 21.10.Ky, 21.10.Hw

1 Introduction

The medium-to heavy-mass Ytterbium (Yb) isotopes located in the rare-earth mass region are well-deformed nuclei that can be populated to very high spin. Much experimental information on even-odd-mass of Yb isotopes has become more abundant [1]-[6]. For the heavier $A = 174$ to 178 nuclei [7], previous work using deep inelastic reactions and Gammasphere have begun to reveal much information about the high-spin behavior of these neutron-rich Yb isotopes. The yrast states in the well deformed rare-earth region have been described by using the projected shell model [8]-[14].

Prior to the present work the level structure of ground band state and low-lying excited states of even-even nuclei has been studied both theoretically and experimentally [15], including the decay, Coulomb excitation and various transfer reactions.

In this study, two calculations for energy levels of $^{170,172,174,176}Yb$ isotopes have been done by using two different models phenomenological model (PhM),

and interacting boson model ($IBM - 1$). Positive parity state energies and the reduced probability of E2 transitions are calculated and compared with the available experimental data. The structure of excited levels is discussed.

2 Theoretical models

The calculations have been performed by using the phenomenological and interacting boson models. In the next subsection, we will explain these models.

2.1 Phenomenological model (PhM)

To analyze the properties of low-lying positive parity states in Yb isotopes, the PhM of [16,17] is used. This model takes into account the mixing of states of the gr^- , β^- , γ^- and $K^\pi = 1^{+-}$ band. The model Hamiltonian is chosen in the following form

$$H = H_{rot}(I^2) + H_{K,K'}^\sigma \quad (1)$$

here $H_{rot}(I^2)$ is rotational part of Hamiltonian,

$$H_{K',K}^\sigma(I) = \omega_K \delta_{K,K'} - \omega_{rot}(I)(j_x)_{K,K'} \xi(I, K) \delta_{K,K' \pm 1} \quad (2)$$

where ω_K bandhead energy of rotational band, $\omega_{rot}(I)$ is the rotational frequency of core, $(j_x)_{K,K'}$ is the matrix elements which describe Coriolis mixture between rotational bands:

$$(j_x)_{gr,1} = -\sqrt{3} \cdot \tau_0, (j_x)_{\beta,1} = -\sqrt{3} \cdot \tau_1, (j_x)_{\gamma,1} = -1 \cdot \tau_2$$

and

$$\xi(I, 0) = 1 \quad \xi(I, 2) = \sqrt{1 - \frac{2}{I(I+1)}}$$

The eigenfunction of Hamiltonian model (1) has the form

$$\begin{aligned} |IMK\rangle = & \left[\frac{2I+1}{16\pi^2} \right]^{\frac{1}{2}} \left\{ \sqrt{2} \Psi_{gr,K}^I D_{MK}^I(\theta) \right. \\ & \left. + \sum_{K'} \frac{\Psi_{K',K}^I}{\sqrt{1+\delta_{K',0}}} \left[D_{M,K'}^I(\theta) b_{K'}^+ + (-1)^{I+K'} D_{M,-K'}^I(\theta) b_{-K'}^+ \right] \right\} |0\rangle \end{aligned} \quad (3)$$

here $\Psi_{K',K}^I$ is the amplitude of mixture of basis states.

Solving the Schrödinger equation one can determine the eigenfunctions and eigenenergies of the positive parity states.

$$(H_{K,\nu}^I - \varepsilon_\nu^I) \Psi_{K,\nu}^I = 0 \quad (4)$$

we can determined the eigenfunctions and eigenenergies of the positive-parity states.

The complete energy of a state is given by

$$E_\nu^I(I) = E_{rot}(I) + \varepsilon_\nu^I(I) \quad (5)$$

The rotating-core energy $E_{rot}(I)$ is calculated by using the Harris parameterizations [18] of the energy and the angular momentum, that is

$$E_{rot}(I) = \frac{1}{2} J_0 \omega_{rot}^2(I) + \frac{3}{4} J_1 \omega_{rot}^4(I) \quad (6)$$

$$\sqrt{I(I+1)} = J_0 \omega_{rot}(I) + J_1 \omega_{rot}^3(I) \quad (7)$$

where j_0 and j_1 are the inertial parameters of the rotational core.

The rotational frequency of the core $\omega_{rot}(I)$ is found by solving the cubic equation (7). This equation has two imaginary roots and one real root. The real root is

$$\omega_{rot}(I) = \left\{ \frac{\tilde{I}}{2j_1} + \left[\left(\frac{j_0}{3j_1} \right)^3 + \left(\frac{\tilde{I}}{2j_1} \right)^2 \right]^{\frac{1}{2}} \right\}^{\frac{1}{3}} + \left\{ \frac{\tilde{I}}{2j_1} - \left[\left(\frac{j_0}{3j_1} \right)^3 + \left(\frac{\tilde{I}}{2j_1} \right)^2 \right]^{\frac{1}{2}} \right\}^{\frac{1}{3}} \quad (8)$$

where $\tilde{I} = \sqrt{I(I+1)}$. Equation (8) gives $\omega_{rot}(I)$ at the given spin I of the core.

2.2 Interacting boson model (*IBM* – 1)

The *IBM* has become one of the most intensively used nuclear models, due to its ability to describe the low-lying collective properties of nuclei across an entire major shell with a Hamiltonian. In the *IBM* – 1 the spectroscopies of low-lying collective properties of even-even nuclei are described in terms of a system of interacting s bosons ($L = 0$) and d bosons ($L = 2$). Furthermore, the model assumes that the structure of low-lying levels is dominated by excitations among the valence particles outside major closed shells. In the particle space the number of proton bosons N_π and neutron bosons N_ϑ is counted from the nearest closed shell, and the resulting total boson number is a strictly conserved quantity. The underlying structure of the six-dimensional unitary group $SU(6)$ of the model leads to a Hamiltonian, capable of describing the three specific types of collective structures with classical geometrical analogues (vibrational [19], rotational [20], and γ -unstable [21]) and also the transitional nuclei [22] whose structures are intermediate. The *IBM* – 1 Hamiltonian can be expressed as [21]

$$\begin{aligned}
H = & \varepsilon_s (s^+ \tilde{s}) + \varepsilon_d (d^+ \tilde{d}) \\
& + \sum_{L=0,2,4} \frac{1}{2} (2L+1)^{\frac{1}{2}} C_L \left[(d^+ \times d^+)^{(L)} (\tilde{d} \times \tilde{d})^{(L)} \right]^{(0)} \\
& + \frac{1}{2} \tilde{\vartheta}_0 \left[(d^+ \times d^+)^{(0)} (\tilde{s} \times \tilde{s})^{(0)} + (s^+ \times s^+)^{(0)} (\tilde{d} \times \tilde{d})^{(0)} \right]^{(0)} \\
& + \frac{1}{\sqrt{2}} \tilde{\vartheta}_2 \left[(d^+ \times d^+)^{(2)} (\tilde{d} \times \tilde{s})^{(2)} + (d^+ \times s^+)^{(2)} (\tilde{d} \times \tilde{d})^{(2)} \right]^{(0)} \\
& + u_2 \left[(d^+ \times s^+)^{(2)} (\tilde{d} \times \tilde{s})^{(2)} \right]^{(0)} + \frac{1}{2} u_0 \left[(s^+ \times s^+)^{(0)} (\tilde{s} \times \tilde{s})^{(0)} \right]^{(0)}
\end{aligned} \tag{9}$$

where (s^\dagger, d^\dagger) and (s, d) are creation and annihilation operators for s and d bosons, respectively.

The $IBM - 1$ Hamiltonian equation (9) can be written in general form as [23]

$$H = \varepsilon n_d + a_0 P^\dagger P + a_1 LL + a_2 QQ + a_3 T3T3 + a_4 T4T4 \tag{10}$$

The full Hamiltonian H contains six adjustable parameters, where $\varepsilon = \varepsilon_d - \varepsilon_s$ is the boson energy and $Q = (d^+ \times \tilde{s} + s^+ \times \tilde{d})^2 + X(d^+ \times \tilde{d})^2$ here $X = CHI$. The parameters a_0, a_1, a_2, a_3 and a_4 designate the strength of the pairing, angular momentum, quadrupole, octupole and hexadecapole interaction between the bosons.

3 Result and Discussion

In this section, the calculated results can be discussed separately for low -lying states of even-even isotopes of Yb , with neutron number from 100 to 106. Our results include energy levels and the reduced probability of $E2-$ transitions.

3.1 Energy levels

To describe the positive parity states in PhM , we determine the model parameters via the following procedure. In accordance with [24], we suppose that, at low spins, the rotational core energy is the same as the energies of the ground band states.

Description of the parameters:

- the inertial parameters j_0 and j_1 of rotational core determined by (6), using the experimental energy of ground band states up to spin $I \leq 10\hbar$;
- headband energy of ground (gr) $^-$, β_1^- and β_2^- band states taken from experimental data, because they are not perturbed by the Coriolis forces at $I = 0$;
- headband energy of γ^- , $K^\pi = 1^+$ bands (ω_γ and ω_{1^+}) and also matrix elements $\langle K | j_x | K' \pm 1 \rangle$ are free parameters of the model. They have been fitted by the least squares method requiring the best agreement between the theoretical energies and experimental data. The fitting parameters of model are given in Table 1.

Also, in the present work the rotational limit of the $IBM - 1$ has been applied to $^{170-176}Yb$, from the ratio $(E(4^+) / E(2^+))$ it has been found that the $^{170-176}Yb$ isotopes are rotational (deformed nuclei) and these nuclei have been successfully treated as exhibiting the $SU(3)$ symmetry of $IBM - 1$. The calculations have been performed with the code *IBM - 1.for* and hence, no distinction is made between neutron and proton bosons. For the analysis of excitation energies in Yb isotopes it we tried to keep to the minimum the number of free parameters in Hamiltonian. The explicit expression of Hamiltonian adopted in calculations is [23].

$$H = a_1 L \cdot L + a_2 Q \cdot Q \quad (11)$$

In framework of the $IBM - 1$, the isotopic chains of Yb with $Z = 70$ nuclei, having a number of proton bosons holes 6, a number of neutron bosons particles

varies from 9 to 11 for $^{170-174}\text{Yb}$, and number of neutron boson hole for ^{176}Yb is 10. In Table 2 shown the coefficient values which we are using in $IBM - 1$. *for*. The comparison of calculated energy levels and experimental data of low-lying states of ^{170}Yb , ^{172}Yb , ^{174}Yb and ^{176}Yb isotopes are presented in the Fig. 1-4, respectively. The PhM calculations are plotted on the left of the experimental data and $IBM - 1$ calculations on the right of it for gr^- , β_1^- and γ_1^- band. The experimental data are taken from [25] for all isotopes of Yb and also from [26]-[29] for $^{170-174}\text{Yb}$ and ^{176}Yb , respectively. From these figures, we can see that our calculated results (energies, spin and parity) in both models are reasonably consistent with experimental data, except γ_1^- band energies in $IBM - 1$ calculations for ^{172}Yb and ^{174}Yb nuclei disagree with the experimental data. Also the phenomenological calculations are in good agreement with the experimental data than from those of $IBM - 1$. In the high spin these figures show that the difference between our calculation and the experimental data. Furthermore the phenomenological model predicts the energies, spin and parity of β_2^- , β_3^- , β_4^- , γ_2^- and 1^+ band and as it shown in the Tables 3-7, respectively. Finally, we believe that the failure to use pairing parameter was the cause of the disagreement between the $IBM - 1$ calculations and experimental data that will be discussed in future studies.

3.2 The Reduced probability of $B(E2)^-$ transitions

In the PhM , with the wave functions calculated by solving the Shrödinger eq. (4), the reduced probabilities of $E2^-$ transitions between states $I_i K_i$ and states

$I_f K_f$ are calculated [16,17] as:

$$\begin{aligned}
B(E2; I_i K_i \rightarrow I_f K_f) = & \left\{ \sqrt{\frac{5}{16\pi}} e Q_0 \left[\Psi_{gr,gr}^{I_f} \Psi_{gr,K_i}^{I_i} C_{I_i 0;20}^{I_f 0} \right. \right. \\
& + \sum_n \Psi_{K_n,gr}^{I_f} \Psi_{K_n,K_i}^{I_i} C_{I_i K_n;20}^{I_f K_n} \left. \right] \\
& + \sqrt{2} \left[\Psi_{gr,gr}^{I_f} \sum_n \frac{(-1)^{K_n} m_{K_n} \Psi_{K_n,K_i}^{I_i}}{\sqrt{1 + \delta_{K_n,0}}} C_{I_i K_n;2-K_n}^{I_f 0} \right. \\
& \left. \left. + \Psi_{gr,K_i}^{I_i} \sum_n \frac{m_{K_n} \Psi_{K_n,gr}^{I_f}}{\sqrt{1 + \delta_{K_n,0}}} C_{I_i K_n;2K_n}^{I_f K_n} \right] \right\}^2 \quad (12)
\end{aligned}$$

where $m_{K_n} = \langle gr | \hat{m}(E2) | K^\pi \rangle$ ($K^\pi = 0^+, 2^+$ and 1^+) are constants to be determined from the experimental data, Q_0 is the internal quadrupole moment of the nucleus, and $C_{I_i K_i;2(K_i+K_f)}^{I_f K_f}$ and are the Clebsch-Gordon coefficients.

Another advantage of the interacting d - boson model is that the matrix elements of the electric quadrupole operator. The reduced matrix elements of the $E2$ operator $\hat{T}(E2)$ has the form [19]-[21]

$$\begin{aligned}
\hat{T}(E2) = & \alpha 2 \left[d^\dagger \tilde{s} + s^\dagger \tilde{d} \right]^2 + \beta 2 \left[d^\dagger \tilde{d} \right]^2 \\
= & \alpha 2 \left\{ \left[d^\dagger \tilde{s} + s^\dagger \tilde{d} \right]^2 + \chi \left[d^\dagger \tilde{d} \right]^2 \right\} = e_B Q \quad (13)
\end{aligned}$$

here $\alpha 2$ and $\beta 2$ are two parameters and $\beta 2 = \chi \alpha 2$, $\alpha 2 = e_B$ (*effective charge*). The values of these parameters are presented in Table 3. Then the $B(E2)$ values are given by

$$B(E2; J_i \rightarrow J_f) = \frac{1}{2J_i + 1} |\langle J_f | \hat{T}(E2) | J_i \rangle|^2 \quad (14)$$

For the calculations of the absolute $B(E2)$ values two parameters $\alpha 2$ and $\beta 2$ of equation (13) are adjusted according to the experimental $B(E2; 2_{gr}^+ \rightarrow 0_{gr}^+)$. Table 8 shows the values of the parameters $\alpha 2$ and $\beta 2$, obtained in the present

calculations. We present our calculated results of the reduced probability of $E2$ -transitions of both models, and the comparison of calculated values of $B(E2)$ transitions with experimental data [30] are given in Table 9 for all nuclei of interest. In general, most of the calculated results in both models are reasonably consistent with the available experimental data, except for few cases that deviate from the experimental data. As mentioned in Table 9 PhM calculations are better than those of $IBM-1$ when compare with the experimental data, except $B(E2; 2_{gr}^+ \rightarrow 0_{gr}^+)$ for ^{170}Yb , ^{174}Yb and ^{176}Yb , $B(E2; 6_{gr}^+ \rightarrow 4_{gr}^+)$ for ^{172}Yb , $B(E2; 4_{gr}^+ \rightarrow 2_{gr}^+)$ and $B(E2; 14_{gr}^+ \rightarrow 12_{gr}^+)$ for ^{174}Yb and also $B(E2; 12_{gr}^+ \rightarrow 10_{gr}^+)$ $B(E2;)$ for ^{170}Yb .

4 Summary

In this paper, energy levels and the reduced probability of $E2^-$ transitions positive parity for $^{170-176}\text{Yb}$ isotopes with neutron numbers between 100 and 106 have been calculated through PhM and $IBM - 1$ calculations using the $IBM.for$ and $IBMT.for$ programs. The predicted low-lying levels ($gr-$, β_1- and γ_1- band) by PhM are in good agreement with the experimental data as compared with those by $IBM - 1$ for all nuclei of interest. In addition, the PhM is successful in predicting the β_2- , β_3- , β_4- , γ_2- and 1^+- band while $IBM - 1$ fails. Also, the 3^+- band is predicted by $IBM - 1$ for ^{172}Yb and ^{174}Yb nuclei. All calculations are compared with the available experimental data. Also, the reduced probability of $E2^-$ transitions of PhM calculations are better than those of $IBM - 1$ when compare with the experimental data, except $B(E2; 2_{gr}^+ \rightarrow 0_{gr}^+)$ for ^{170}Yb , ^{174}Yb and ^{176}Yb , $B(E2; 6_{gr}^+ \rightarrow 4_{gr}^+)$ for ^{172}Yb , $B(E2; 4_{gr}^+ \rightarrow 2_{gr}^+)$ and $B(E2; 14_{gr}^+ \rightarrow 12_{gr}^+)$ for ^{174}Yb and also $B(E2; 12_{gr}^+ \rightarrow 10_{gr}^+)$ $B(E2;)$ for ^{170}Yb .

Acknowledgements

This work has been financial supported by IIUM University Research Grant (Type B) EDW B13-034-0919 and MOHE Fundamental Research Grant Scheme FRGS13-077-0315. We thank the Islamic Development Bank (IDB) for supporting this work under scholarships Nos. 36/11201905/35/IRQ/D31 and 37/IRQ/P30. The author A. A. Okhunov is grateful to Prof. Ph.N. Usmanov for useful discussion and exchange ideas.

References

1. J N Mo et al. *Nucl. Phys. A* **472** 295 (1987)
2. S Jonsson, N Roy, H Ryde, W Walus et al. *Nucl. Phys. A* **449** 537 (1986)

3. E M Beck, J C.Bcelar, M A Deleplanque, R M Diamond et al. *Nucl. Phys. A* **464** 472 (1987)
4. T Byrski et al. *Nucl. Phys. A* **474** 193 (1987)
5. M P Fewell et al. *Phys. Rev. C* **37** 101 (1988)
6. C Granja, S Posíšil, R E Chrien and S.A.Telezhnikovc *Nucl. Phys. A* **757** 287 (2005)
7. I Y Lee et al. *Phys. Rev. C* **56** 753 (1997)
8. K Hara and S Iwasaki *Nucl. Phys. A* **348** 200 (1980)
9. K Hara and S Iwasaki *Nucl. Phys. A* **430** 175 (1984)
10. K Hara and Y Sun *Nucl. Phys. A* **529** 445 (1991)
11. K Hara and Y Sun *Nucl. Phys. A* **531** 221 (1991)
12. K Hara and Y Sun *Nucl. Phys. A* **537** 77 (1992)
13. Y Sun and J L Egido *Nucl. Phys. A* **580** 1 (1994)
14. D E Archer et al. *Phys. Rev. C* **57** 2924 (1998)
15. W Gelletly et al. *J. Phys. G: Nucle. Phys.* **13**, 69 (1987)
16. Ph N Usmanov and I N Mikhailov *Phys. Part. Nucl. Lett.* **28**, 348 (1997)
[*Fiz.Elem.Chastits At. Yadra* **28**, 887 (1997)]
17. Ph N Usmanov, A A Okhunov, U S Salikhbaev and A Vdovin *Phys. Part. Nucl. Lett.* **7**, 185 (2010) [*Fiz.Elem.Chastits At. Yadra* **159**, 306 (2010)]
18. S M Harris *Phys. Rev. B* **138** 509, (1965)
19. A Arima and F Iachello *Ann. Phys. NY* **99** 253 (1976)
20. A Arima and F Iachello *Ann. Phys. NY* **111** 201 (1978)
21. A Arima and F Iachello *Ann. Phys. NY* **123** 468 (1979)
22. O Scholten, F Iachello, and A Arima *Ann. Phys. NY* **115** 325 (1978)
23. R F Casten and D D Warner *Rev. Mod. Phys.* **60** 389 (1988)
24. R Bengtsson and S Fraundorf *Nucl.Phys. A* **327** 139 (1979)
25. R B Begzhanov et al. *Handbook on Nuclear Physics Vol 1.2* (Tashkent: FAN) (1989)
26. C M Baglin *Nucl. Data. Sheets* **96** 611 (2002)
27. B Singh *Nucl. Data. Sheets* **75** 199 (1995)

28. E Browne and H Junde *Nucl. Data. Sheets* **87** 15 (1999)
29. M S Basunia *Nucl. Data. Sheets* **107** 791 (2006)
30. <http://www.nndc.bnl.gov/chart/getENSDFDatasets.jsp>

List of Table captions

Table 1 The used parameters of PhM to calculate energy of low excited states in Yb isotopes.

Table 2 The used parameters of $IBM - 1$ to calculate energy of excited states in Yb isotopes.

Table 3 The value of parameters obtained from $\hat{T}(E2)$ operator in program IBMT.for for calculate the absolute values of $B(E2)$ in (in eb).

Table 4 The energy levels of β_2- band of Yb isotopes (in MeV).

Table 5 The energy levels of β_3- band of Yb isotopes (in MeV).

Table 6 The energy levels of β_4- band of Yb isotopes (in MeV).

Table 7 The energy levels of γ_2- band of Yb isotopes (in MeV).

Table 8 The energy levels of $1^{+}-$ band of Yb isotopes (in MeV).

Table 9 The values of $B(E2)-$ transitions isotopes of Yb (in $W.u.$).

Table 1.

A	$(j_x)_{gr,1}$	$(j_x)_{\beta_1,1}$	$(j_x)_{\beta_2,1}$	$(j_x)_{\beta_3,1}$	$(j_x)_{\beta_4,1}$	$(j_x)_{\gamma_1,1}$	$(j_x)_{\gamma_2,1}$	Q_0
170	0.186	0.394	0.659	0.908	–	0.728	–	780 (30)
172	0.275	0.978	0.718	0.110	0.300	0.325	0.210	791 (18)
174	0.185	0.400	0.250	0.150	0.200	0.085	0.100	782 (24)
176	0.200	0.540	0.400	0.100	–	0.090	–	759 (3)

Note: $(j_x)_{\kappa',\kappa}$ – are matrix elements of the Coriolis interactions and Q_0 – is intrinsic quadrupole moment of the nucleus (in fm^2 units) taken from [25].

Table 2.

A	a_1	a_2	CHI
170	0.0094	-0.0120	-1.30
172	0.0091	-0.0112	-1.20
174	0.0084	-0.0150	-1.24
176	0.0089	-0.0126	-1.30

Table 3.

A	α_2	β_2
170	0.1060	-0.140
172	0.1037	-0.137
174	0.0960	-0.126
176	0.0980	-0.129

Table 4.

	^{170}Yb		^{172}Yb		^{174}Yb		^{176}Yb	
I	Exp.[25,26]	PhM	Exp.[25,27]	PhM	Exp.[25,28]	PhM	Exp.[25,29]	PhM
0^+	1.228	1.228	1.404	1.404	1.885	1.885	1.518	1.518
2^+	1.306	1.313	1.476	1.483	1.958	1.962	1.610	1.601
4^+	—	1.507	1.632	1.666	2.123	2.140	—	1.792
6^+	—	1.804	—	1.947	—	2.414	—	2.086
8^+	—	2.195	—	2.317	—	2.770	—	2.476
10^+	—	2.669	—	2.769	—	3.221	—	2.954
12^+	—	3.220	—	3.295	—	3.740	—	3.512

Table 5.

	^{170}Yb		^{172}Yb		^{174}Yb		^{176}Yb	
I	Exp.[25,26]	PhM	Exp.[25,27]	PhM	Exp.[25,28]	PhM	Exp.[25,29]	PhM
0^+	1.479	1.479	1.794	1.794	2.113	2.110	1.779	1.779
2^+	1.534	1.564	1.849	1.873	2.172	2.178	—	1.862
4^+	1.667	1.758	1.975	2.056	2.336	2.356	—	2.053
6^+	—	2.055	2.156	2.156	—	2.630	—	2.347
8^+	—	2.446	—	2.707	—	2.993	—	2.737
10^+	—	2.920	—	3.159	—	3.437	—	3.215
12^+	—	3.471	—	3.685	—	3.956	—	3.773

Table 6.

I	^{172}Yb		^{174}Yb	
	Exp.[25,27]	PhM	Exp.[25,28]	PhM
0^+	1.894	1.894	2.821	2.821
2^+	1.956	1.973	–	2.898
4^+	2.100	2.156	–	3.076
6^+	–	2.437	–	3.350
8^+	–	2.807	–	3.713
10^+	–	3.259	–	4.157
12^+	–	3.785	–	4.676

Table 7.

I	^{172}Yb		^{174}Yb	
	Exp.[25,27]	<i>PhM</i>	Exp.[25,28]	<i>PhM</i>
2^+	1.608	1.619	2.728	2.727
3^+	1.700	1.698	2.793	2.804
4^+	1.803	1.802	2.882	2.905
5^+	1.926	1.931	–	3.031
6^+	2.075	2.083	–	3.179
7^+	–	2.257	–	3.350
8^+	–	2.453	–	3.542
9^+	–	2.669	–	3.754
10^+	–	2.905	–	3.986
11^+	–	3.159	–	4.236
12^+	–	3.431	–	4.505
13^+	–	3.720	–	4.791
14^+	–	4.026	–	5.093

Table 8.

I	^{170}Yb		^{172}Yb		^{174}Yb		^{176}Yb	
	Exp.[25,26]	PhM	Exp.[25,27]	PhM	Exp.[25,28]	PhM	Exp.[25,29]	PhM
1^+	1.606	1.605	2.009	2.006	1.624	1.605	1.819	1.818
2^+	1.832	1.662	2.047	2.059	1.674	1.657	1.867	1.874
3^+	—	1.746	2.109	2.138	1.733	1.734	—	1.956
4^+	—	1.856	2.193	2.242	1.859	1.835	—	2.065
5^+	—	1.993	—	2.371	—	1.961	—	2.200
6^+	—	2.153	—	2.523	—	2.109	—	2.359
7^+	—	2.337	—	2.697	—	2.280	—	2.542
8^+	—	2.544	—	2.893	—	2.472	—	2.749
9^+	—	2.771	—	3.109	—	2.684	—	2.977
10^+	—	3.018	—	3.345	—	2.916	—	3.227
11^+	—	3.285	—	3.599	—	3.166	—	3.496
12^+	—	3.569	—	3.871	—	3.435	—	3.785
13^+	—	3.871	—	4.160	—	3.721	—	4.093
14^+	—	4.190	—	4.466	—	4.023	—	4.419

List of figure captions

Figure 1 The comparison of calculation energy values by PhM and $IBM-1$ with experimental data for ^{170}Yb .

Figure 2 The comparison of calculation energy values by PhM and $IBM-1$ with experimental data for ^{172}Yb .

Figure 3 The comparison of calculation energy values by PhM and $IBM-1$ with experimental data for ^{174}Yb .

Figure 4 The comparison of calculation energy values by PhM and $IBM-1$ with experimental data for ^{176}Yb .

Table 9.

^{170}Yb				^{172}Yb			
$I_i K_i \rightarrow I_f K_f$	Exp.[30]	PhM	$IBM - 1$	Exp.[30]	PhM	$IBM - 1$	
$2_{gr}^+ \rightarrow 0_{gr}^+$	201(6)	216	198.543	212(2)	212	211.689	
$4_{gr}^+ \rightarrow 2_{gr}^+$	—	309	280.768	301(20)	303	299.697	
$6_{gr}^+ \rightarrow 4_{gr}^+$	—	340	303.549	320(30)	334	324.746	
$8_{gr}^+ \rightarrow 6_{gr}^+$	360(30)	356	309.178	400(40)	350	331.835	
$10_{gr}^+ \rightarrow 8_{gr}^+$	356(25)	366	306.15	375(23)	359	329.971	
$12_{gr}^+ \rightarrow 10_{gr}^+$	268(21)	372	296.956	430(60)	366	322.160	
$14_{gr}^+ \rightarrow 12_{gr}^+$	—	377	283.181	394_{-45}^{+60}	370	309.724	
$16_{gr}^+ \rightarrow 14_{gr}^+$	—	381	265.349	—	374	293.311	
$18_{gr}^+ \rightarrow 16_{gr}^+$	—	383	243.819	—	376	273.310	
$20_{gr}^+ \rightarrow 18_{gr}^+$	—	386	218.751	—	379	249.967	
^{174}Yb				^{176}Yb			
$I_i K_i \rightarrow I_f K_f$	Exp.[30]	PhM	$IBM - 1$	Exp.[30]	PhM	$IBM - 1$	
$2_{gr}^+ \rightarrow 0_{gr}^+$	201(7)	205	199.908	183(7)	184	182.916	
$4_{gr}^+ \rightarrow 2_{gr}^+$	280(9)	294	283.321	270(25)	263	258.969	
$6_{gr}^+ \rightarrow 4_{gr}^+$	370(50)	324	307.532	298(22)	290	280.618	
$8_{gr}^+ \rightarrow 6_{gr}^+$	388(21)	339	315.122	300(5)	303	286.743	
$10_{gr}^+ \rightarrow 8_{gr}^+$	335(22)	348	314.533	—	312	285.139	
$12_{gr}^+ \rightarrow 10_{gr}^+$	369(23)	354	308.624	—	317	278.384	
$14_{gr}^+ \rightarrow 12_{gr}^+$	320(8)	359	298.941	—	321	267.636	
$16_{gr}^+ \rightarrow 14_{gr}^+$	—	362	285.192	—	324	253.459	
$18_{gr}^+ \rightarrow 16_{gr}^+$	—	365	268.659	—	327	236.177	
$20_{gr}^+ \rightarrow 18_{gr}^+$	—	367	249.249	—	328	215.995	

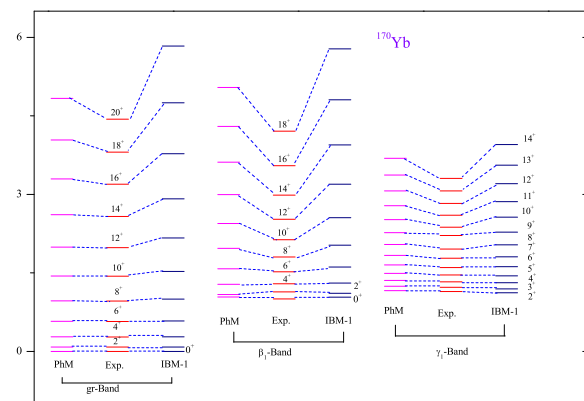


Fig. 1.

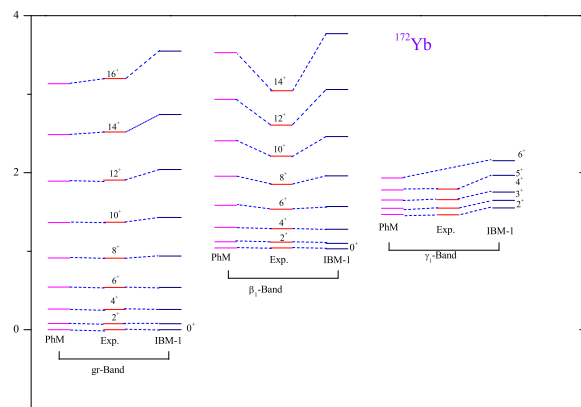


Fig. 2.

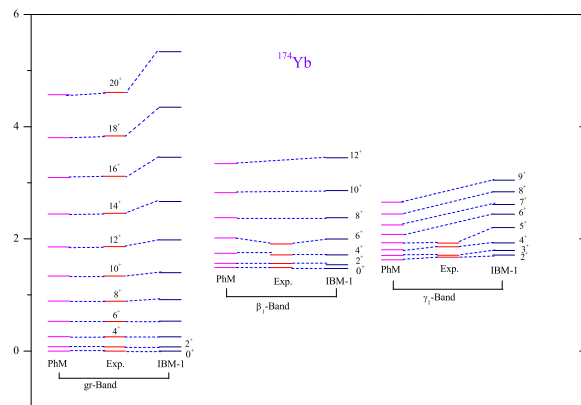


Fig. 3.

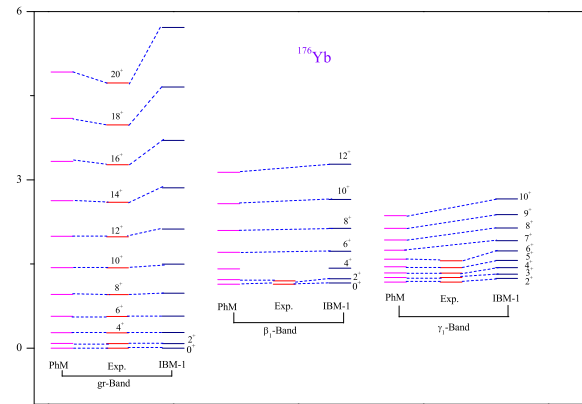


Fig. 4.